

REPORT DOCUMENTATION PAGE			Form Approved OMB NO. 0704-0188		
<p>The public reporting burden for this collection of information is estimated to average 1 hour per response, including the time for reviewing instructions, searching existing data sources, gathering and maintaining the data needed, and completing and reviewing the collection of information. Send comments regarding this burden estimate or any other aspect of this collection of information, including suggestions for reducing this burden, to Washington Headquarters Services, Directorate for Information Operations and Reports, 1215 Jefferson Davis Highway, Suite 1204, Arlington VA, 22202-4302. Respondents should be aware that notwithstanding any other provision of law, no person shall be subject to any penalty for failing to comply with a collection of information if it does not display a currently valid OMB control number.</p> <p>PLEASE DO NOT RETURN YOUR FORM TO THE ABOVE ADDRESS.</p>					
1. REPORT DATE (DD-MM-YYYY) 23-12-2012		2. REPORT TYPE Final Report		3. DATES COVERED (From - To) 1-May-2009 - 30-Apr-2012	
4. TITLE AND SUBTITLE Final Report			5a. CONTRACT NUMBER W911NF-09-1-0111		
			5b. GRANT NUMBER		
			5c. PROGRAM ELEMENT NUMBER 611102		
6. AUTHORS Richard A. Regueiro			5d. PROJECT NUMBER		
			5e. TASK NUMBER		
			5f. WORK UNIT NUMBER		
7. PERFORMING ORGANIZATION NAMES AND ADDRESSES University of Colorado - Boulder The Regents of the University of Colorado Office of Contracts and Grants Boulder, CO 80309 -0572			8. PERFORMING ORGANIZATION REPORT NUMBER		
9. SPONSORING/MONITORING AGENCY NAME(S) AND ADDRESS(ES) U.S. Army Research Office P.O. Box 12211 Research Triangle Park, NC 27709-2211			10. SPONSOR/MONITOR'S ACRONYM(S) ARO		
			11. SPONSOR/MONITOR'S REPORT NUMBER(S) 56031-EG.7		
12. DISTRIBUTION AVAILABILITY STATEMENT Approved for Public Release; Distribution Unlimited					
13. SUPPLEMENTARY NOTES The views, opinions and/or findings contained in this report are those of the author(s) and should not be construed as an official Department of the Army position, policy or decision, unless so designated by other documentation.					
14. ABSTRACT Using solely grain-scale physics-based simulation methods, it is too computationally intensive to account for both (I) global initial boundary value problem (IBVP) conditions, and (II) grain-scale material behavior, to understand fundamentally the mechanics of dynamic failure in bound particulate materials. The objective of the proposed research is to achieve this understanding by accounting simultaneously for grain-scale physics and macro-scale continuum IBVP conditions. To achieve the proposed objective, a concurrent computational multi-scale modeling					
15. SUBJECT TERMS finite strain, micromorphic, three-dimensional mixed finite element implementation, DE-FE overlap coupling					
16. SECURITY CLASSIFICATION OF:		17. LIMITATION OF ABSTRACT		15. NUMBER OF PAGES	19a. NAME OF RESPONSIBLE PERSON
a. REPORT UU	b. ABSTRACT UU	c. THIS PAGE UU	UU		Richard Regueiro
					19b. TELEPHONE NUMBER 303-492-8026

Report Title

Final Report

ABSTRACT

Using solely grain-scale physics-based simulation methods, it is too computationally intensive to account for both (I) global initial boundary value problem (IBVP) conditions, and (II) grain-scale material behavior, to understand fundamentally the mechanics of dynamic failure in bound particulate materials. The objective of the proposed research is to achieve this understanding by accounting simultaneously for grain-scale physics and macro-scale continuum IBVP conditions. To achieve the proposed objective, a concurrent computational multi-scale modeling approach will be developed that involves the following 3 features: (1) coupling regions of micromorphic continuum finite element to an 'open window' on the particulate micro-structure where localized deformation nucleates and an interface with a deformable solid body could exist; (2) converting to discrete element fragmentation modeling in micro-structural regions; and (3) adapting numerically grain-scale resolution over the material domain. The desired result is to enable a more complete understanding of the role of grain-scale physics on the thermo-mechanical properties and performance of heterogeneous bound particulate materials of interest to the Army. The contribution will be demonstrated by working with Army researchers in the Impact Physics Branch during onsite visits and through an open-source research code Tahoe where the concurrent multi-scale model will be implemented.

Enter List of papers submitted or published that acknowledge ARO support from the start of the project to the date of this printing. List the papers, including journal references, in the following categories:

(a) Papers published in peer-reviewed journals (N/A for none)

<u>Received</u>	<u>Paper</u>
08/29/2011	2.00 R. A. Regueiro, V. Isbuga. Length scale effects in finite strain micromorphic linear isotropic elasticity: finite element analysis of three-dimensional cubical microindentation, Proceedings of the Institution of Mechanical Engineers, Part N: Journal of Nanoengineering and Nanosystems, (07 2011): 0. doi: 10.1177/1740349911412850
08/29/2011	3.00 Volkan Isbuga, Richard A. Regueiro. Three-dimensional finite element analysis of finite deformation micromorphic linear isotropic elasticity, International Journal of Engineering Science, (05 2011): 0. doi: 10.1016/j.ijengsci.2011.04.006
TOTAL:	2

Number of Papers published in peer-reviewed journals:

(b) Papers published in non-peer-reviewed journals (N/A for none)

<u>Received</u>	<u>Paper</u>
-----------------	--------------

TOTAL:

Number of Papers published in non peer-reviewed journals:

(c) Presentations

October 2012, Concurrent multiscale computational modeling of particulate materials: (i) 3D ellipsoidal DEM of X-ray CT sand assemblies, (ii) overlap coupling of DEM and micromorphic FEM, SES 2012, GeorgiaTech, Atlanta.

September 2012, Total Lagrangian Nonlinear Finite Element Analysis of Finite Strain Micromorphic Pressure-Sensitive Elastoplasticity, ECCOMAS 2012, University of Vienna, Austria.

Number of Presentations: 2.00

Non Peer-Reviewed Conference Proceeding publications (other than abstracts):

<u>Received</u>	<u>Paper</u>	
12/23/2012	5.00	Volkan Isbuga, Richard Regueiro. FINITE ELEMENT ANALYSIS OF FINITE STRAIN MICROMORPHIC ISOTROPIC ELASTICITY AND DRUCKER-PRAGER PLASTICITY, 2012 ASCE Joint Conference of the Engineering Mechanics Institute. 2012/06/18 02:00:00, . . . ,
TOTAL:	1	

Number of Non Peer-Reviewed Conference Proceeding publications (other than abstracts):

Peer-Reviewed Conference Proceeding publications (other than abstracts):

<u>Received</u>	<u>Paper</u>	
08/29/2011	1.00	Richard A. Regueiro, Beichuan Yan. Coupling discrete elements and micropolar continuum through an overlapping region, GeoFrontiers 2011. 2011/03/14 02:00:00, . . . ,
TOTAL:	1	

Number of Peer-Reviewed Conference Proceeding publications (other than abstracts):

(d) Manuscripts

Received Paper

TOTAL:

Number of Manuscripts:

Books

Received Paper

12/23/2012 6.00 Richard Regueiro, Beichuan yan. Computational homogenization and partial overlap coupling between micropolar elastic continuum finite elements and elastic spherical discrete elements in one dimension, Boca Raton, FL: Pan Stanford Publishing Co., (02 2013)

TOTAL: **1**

Patents Submitted

Patents Awarded

Awards

Graduate Students

<u>NAME</u>	<u>PERCENT SUPPORTED</u>	Discipline
Volkan Isbuga	0.50	
FTE Equivalent:	0.50	
Total Number:	1	

Names of Post Doctorates

<u>NAME</u>	<u>PERCENT SUPPORTED</u>
Volkan Isbuga	0.10
FTE Equivalent:	0.10
Total Number:	1

Names of Faculty Supported

<u>NAME</u>	<u>PERCENT SUPPORTED</u>	National Academy Member
Richard Regueiro	0.08	
FTE Equivalent:	0.08	
Total Number:	1	

Names of Under Graduate students supported

<u>NAME</u>	<u>PERCENT SUPPORTED</u>
FTE Equivalent:	
Total Number:	

Student Metrics

This section only applies to graduating undergraduates supported by this agreement in this reporting period

- The number of undergraduates funded by this agreement who graduated during this period: 0.00
- The number of undergraduates funded by this agreement who graduated during this period with a degree in science, mathematics, engineering, or technology fields:..... 0.00
- The number of undergraduates funded by your agreement who graduated during this period and will continue to pursue a graduate or Ph.D. degree in science, mathematics, engineering, or technology fields:..... 0.00
- Number of graduating undergraduates who achieved a 3.5 GPA to 4.0 (4.0 max scale):..... 0.00
- Number of graduating undergraduates funded by a DoD funded Center of Excellence grant for Education, Research and Engineering:..... 0.00
- The number of undergraduates funded by your agreement who graduated during this period and intend to work for the Department of Defense 0.00
- The number of undergraduates funded by your agreement who graduated during this period and will receive scholarships or fellowships for further studies in science, mathematics, engineering or technology fields: 0.00

Names of Personnel receiving masters degrees

<u>NAME</u>
Total Number:

Names of personnel receiving PHDs

<u>NAME</u>
Volkan Isbuga
Total Number:
1

Names of other research staff

<u>NAME</u>	<u>PERCENT SUPPORTED</u>
FTE Equivalent:	
Total Number:	

Sub Contractors (DD882)

Inventions (DD882)

Scientific Progress

See attachment

Technology Transfer

Scientific Progress and Accomplishments

contract/grant number: W911NF-09-1-0111

ARO proposal number: 56031-EG

December 31, 2012

Richard A. Regueiro

Associate Professor

Department of Civil, Environmental, and Architectural Engineering
University of Colorado, Boulder

The outline of this section of the final report is as follows:

1. overview of micromorphic finite element (FE) results presented in various published journal articles [Isbuga and Regueiro, 2011, Regueiro and Isbuga, 2011, Isbuga and Regueiro, 2012] and PhD thesis [Isbuga, 2012] funded by this research grant;
2. overview of discrete element and micropolar continuum finite element coupling in one dimension, and numerical results [Regueiro and Yan, 2013];
3. formulation of overlap coupling for grain-FE scale and micromorphic continuum FE scale (two methods);
4. overview of adaptivity approach;
5. summary of future research

1 Overview of micromorphic finite element (FE) results

This section summarizes briefly the micromorphic finite element (FE) results presented in various published journal articles [Isbuga and Regueiro, 2011, Regueiro and Isbuga, 2011, Isbuga and Regueiro, 2012] and PhD thesis [Isbuga, 2012] funded by this research grant. More details can be found in the cited articles and thesis, provided as attachments.

The papers Isbuga and Regueiro [2011], Regueiro and Isbuga [2011] focussed on the finite strain, materially linear isotropic elastic, three-dimensional finite element implementation and numerical results using Tahoe. We showed that the implementation is convergent with respect to spatial discretization (i.e., mesh size), even in the presence of a boundary layer. Upon increasing elastic length scale, the boundary layer was found to become less sharp. For pressure-sensitive Drucker-Prager elasto-plasticity [Isbuga and Regueiro, 2012, Isbuga, 2012], it was found that choice of micromorphic elastic parameters in conjunction with plastic strength parameters will influence the stress paths and, in turn, yielding. The boundary conditions on the micro-displacement tensor Φ^h had a significant influence on the results. A plastic length scale term has not yet been implemented, and it is anticipated that this will influence the numerical results where there is a gradient of an internal state variable (ISV) in a region of large deformation.

2 Overview of discrete element and micropolar continuum finite element coupling in one dimension, and numerical results

The ultimate problem of interest is shown in Fig.1. The discrete element (DE) and/or finite element (FE) representation of the particulate micro-structure is intentionally not shown in order not to clutter the drawing of the micro-structure. The grains (binder matrix not shown) of the micro-structure are ‘meshed’ using DEs and/or FEs with cohesive surface elements (CSEs). The open circles denote continuum FE nodes that have prescribed degrees of freedom (dofs) $\hat{\mathbf{D}}$ based on the underlying grain-scale response, while the solid circles denote continuum FE nodes that have free dofs \mathbf{D} governed by the micromorphic continuum model. We intentionally leave an ‘open window’ (i.e., Direct Numerical Simulation (DNS) region) on the particulate micro-structural mesh in order to model dynamic failure. If the continuum mesh overlays the whole particulate micro-structural region, as in Klein and Zimmerman [2006] for atomistic-continuum coupling, then the continuum FEs would eventually become too deformed by following the micro-structural motion during fragmentation. The blue-dashed box at the bottom-center of the illustration is a micromorphic continuum FE region that can be converted to a DNS region for adaptive high-fidelity material modeling as the projectile penetrates the target.

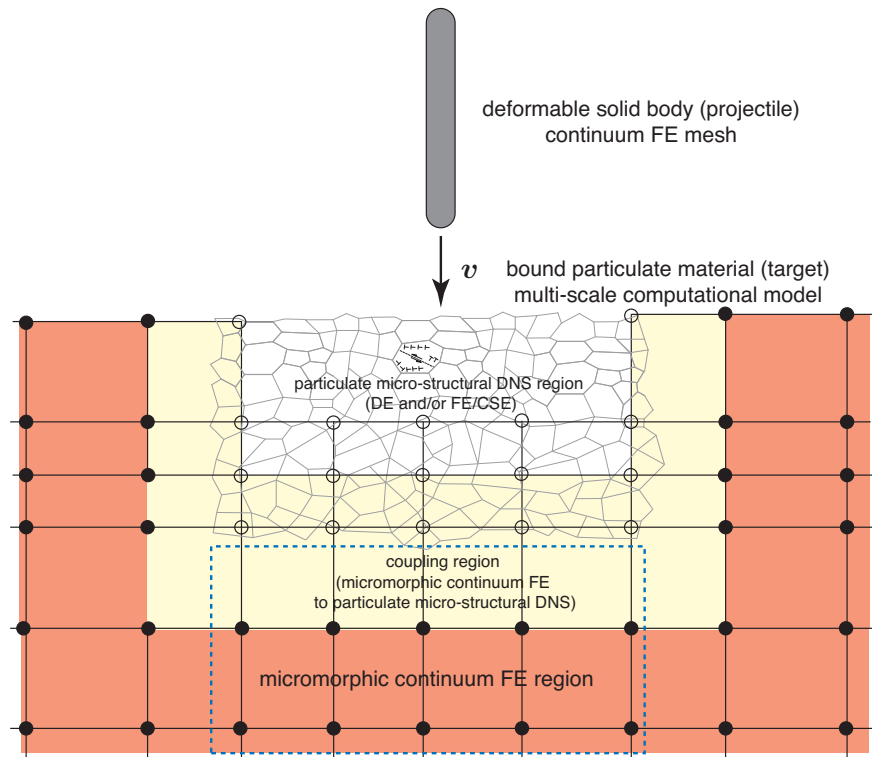


Figure 1. 2D illustration of concurrent computational multi-scale modeling approach in the contact interface region between a bound particulate material (e.g., ceramic target) and deformable solid body (e.g., refractory metal projectile).

In order to simplify the problem, we consider the compression and shear of the interface of DNS region with the micromorphic continuum FE region as a 1D overlap problem between glued, nonlinear elastic DEs, and micropolar elastic continuum FE [Regueiro and Yan, 2013]. Details may be found in Regueiro and Yan [2013]. In summary, we learned that the coupling methodology generally works for quasi-statics between DEs and FEs, but the 1D problem is too “discrete” to yield the results we expect, i.e., no influence of overlap coupling region. This is because shear and rotational degrees of freedom are coupled in the DE and FE formulations, and thus upon shearing the end of the DE string of particles, a ratcheting rotational mode is propagated through the DE string and into the FE continuum domain where it is smoothed out. We are working on extending this coupling method to include inertia terms (dynamics), and also to couple grain-FE to micromorphic FE for 2D and 3D problems.

3 Formulation of overlap coupling for grain-FE scale and micromorphic continuum FE scale

Two coupling approaches in Sections 3.1 and 3.2 were considered in this research. Coupling Approach 1 is implemented with numerical results discussed in Section 2. Coupling Approach 1 is based on the “bridging-scale decomposition” in Wagner and Liu [2003], Kadwaki and Liu [2004], Klein and Zimmerman [2006], and Coupling Approach 2 is based on the “bridging domain method” in Xiao and Belytschko [2004]. Coupling Approach 1 couples the DNS and micromorphic FE dofs directly through interpolation functions in the overlap region, and partitions the energy through scaling factors within each term of the energy (kinetic and potential energies). Coupling Approach 2 partitions the energies through a scalar distance function $\omega(\mathbf{X})$ (describing the width of the overlapping domain), and uses Lagrange multipliers to constrain the DNS displacements to the micromorphic continuum FE displacements in the overlapping domain.

3.1 Coupling Approach 1:

It is assumed that the micromorphic continuum-FE mesh covers the domain of the problem in which the bound particulate mechanics is not dominant, whereas in regions of significant grain-matrix debonding or intra-granular cracking leading to a macro-crack, a grain-scale mechanics representation is used (e.g., grain-FE, grain-DE-FE, grain peridynamics [Silling, 2000]) in Fig.2.

3.1.1 3D Kinematics

Here, a summary of the kinematics of the coupled regions is given for general 3-D kinematics, following the illustration shown in Fig.2. It is assumed that the micromorphic continuum finite element (FE) mesh covers the domain of the problem in which the material is not fragmenting, whereas in regions of fracture and fragmentation, a DNS (e.g., DE/FE/CSE, or peridynamics [Silling, 2000]) representation can be used. In Fig.2, discrete domains are defined, where the yellow background denotes the FE overlap region $\tilde{\mathcal{B}}^h$ with underlying ghost DNS nodes, brown the micromorphic FE continuum region $\bar{\mathcal{B}}^h$ with no underlying DNS, and white background the free DNS region $\hat{\mathcal{B}}^h \cup \mathcal{B}^{DNS}$. In summary, the finite element domain \mathcal{B}^h is the union of pure micromorphic continuum FE domain $\bar{\mathcal{B}}^h$, overlapping FE domain with underlying ghost DNS nodes $\tilde{\mathcal{B}}^h$, and overlapping FE domain with underlying free DNS nodes $\hat{\mathcal{B}}^h$, such that $\mathcal{B}^h = \bar{\mathcal{B}}^h \cup \tilde{\mathcal{B}}^h \cup \hat{\mathcal{B}}^h$. The pure DNS domain with no overlapping FE domain (i.e., the ‘open-window’) is indicated by \mathcal{B}^{DNS} . The goal is to have the overlap region $\hat{\mathcal{B}}^h \cup \bar{\mathcal{B}}^h$ as close to the region of interest (e.g., penetrator skin) as to minimize the number of DNS nodes, and, thus, computational effort. Following some of the same notation presented in Klein and Zimmerman [2006], we define a generalized dof vector $\check{\mathbf{Q}}$ for DNS displacements in the system as

$$\check{\mathbf{Q}} = [\mathbf{q}_\alpha, \mathbf{q}_\beta, \dots, \mathbf{q}_\gamma]^T, \quad \alpha, \beta, \dots, \gamma \in \check{\mathcal{A}} \quad (1)$$

where \mathbf{q}_α is the displacement vector of DNS node α , and $\check{\mathcal{A}}$ is the set of all DNS nodes. Likewise, the micromorphic finite element nodal displacements and micro-displacements are

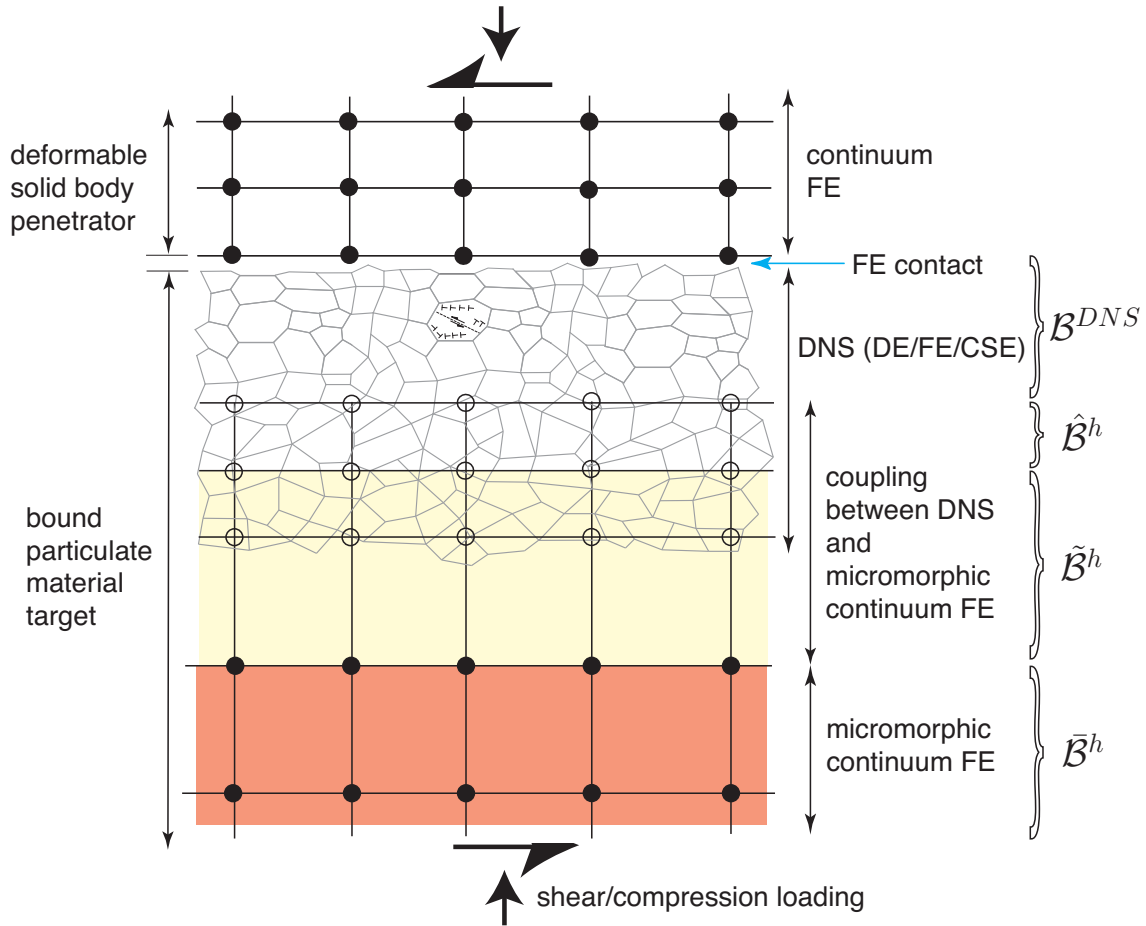


Figure 2. Two-dimensional illustration of the Coupling Approach 1 between grain-FE DNS and micromorphic FE continuum regions.

written as

$$\check{\mathbf{D}} = [d_a, d_b, \dots, d_c, \phi_d, \phi_e, \dots, \phi_f]^T \quad (2)$$

$$a, b, \dots, c \in \check{\mathcal{N}}, \quad d, e, \dots, f \in \check{\mathcal{M}}$$

where \mathbf{d}_a is the displacement vector of node a , ϕ_d is the micro-displacement tensor in vector form of node d , $\check{\mathcal{N}}$ is the set of all nodes, and $\check{\mathcal{M}}$ is the set of micromorphic finite element nodes with micro-displacement tensor degrees of freedom, where $\check{\mathcal{M}} \subset \check{\mathcal{N}}$. In order to satisfy the boundary conditions for both regions, the motion of the DNS nodes in the overlap region (referred to as “ghost DNS nodes,” cf. Fig.2) is prescribed by the micromorphic continuum displacement and micro-displacement fields, and written as

$$\hat{\mathbf{Q}} = [q_\alpha, q_\beta, \dots, q_\gamma]^T, \quad \alpha, \beta, \dots, \gamma \in \hat{\mathcal{A}}, \quad \hat{\mathcal{A}} \in \tilde{\mathcal{B}}^h \quad (3)$$

while the unprescribed (or free) DNS nodal displacements are

$$\mathbf{Q} = [q_\delta, q_\epsilon, \dots, q_\eta]^T, \quad \delta, \epsilon, \dots, \eta \in \mathcal{A}, \quad \mathcal{A} \in \hat{\mathcal{B}}^h \cup \mathcal{B}^{DNS} \quad (4)$$

where $\widehat{\mathcal{A}} \cup \mathcal{A} = \check{\mathcal{A}}$ and $\widehat{\mathcal{A}} \cap \mathcal{A} = \emptyset$. Likewise, the displacements and micro-displacement tensor components of nodes overlaying the DNS region are prescribed by the DNS motion and written as

$$\begin{aligned} \widehat{\mathbf{D}} &= [\mathbf{d}_a, \mathbf{d}_b, \dots, \mathbf{d}_c, \phi_d, \phi_e, \dots, \phi_f]^T \\ a, b, \dots, c &\in \widehat{\mathcal{N}}, \quad d, e, \dots, f \in \widehat{\mathcal{M}} \\ \widehat{\mathcal{N}}, \widehat{\mathcal{M}} &\in \widetilde{\mathcal{B}}^h \cup \widehat{\mathcal{B}}^h \end{aligned} \quad (5)$$

while the unprescribed (or free) nodal displacements and micro-displacements are

$$\begin{aligned} \mathbf{D} &= [\mathbf{d}_m, \mathbf{d}_n, \dots, \mathbf{d}_s, \phi_t, \phi_u, \dots, \phi_v]^T \\ m, n, \dots, s &\in \mathcal{N}, \quad t, u, \dots, v \in \mathcal{M} \\ \mathcal{N}, \mathcal{M} &\in \widetilde{\mathcal{B}}^h \cup \widehat{\mathcal{B}}^h \end{aligned} \quad (6)$$

where $\widehat{\mathcal{N}} \cup \mathcal{N} = \check{\mathcal{N}}$, $\widehat{\mathcal{N}} \cap \mathcal{N} = \emptyset$, $\widehat{\mathcal{M}} \cup \mathcal{M} = \check{\mathcal{M}}$, and $\widehat{\mathcal{M}} \cap \mathcal{M} = \emptyset$. Referring to Fig.2, the prescribed DNS nodal dofs $\widehat{\mathcal{Q}}$ can be viewed as boundary constraints on the free DNS region, and likewise the prescribed micromorphic finite element nodal displacements and micro-displacements $\widehat{\mathbf{D}}$ can be viewed as boundary constraints on the finite element mesh in the overlap region.

In general, the displacement vector of a DNS node α can be represented by the finite element interpolation of the micromorphic continuum macro-displacement field \mathbf{u}^h and micro-displacement tensor field Φ^h evaluated at the DNS node in the reference configuration \mathbf{X}_α^h , such that

$$\mathbf{u}^h(\mathbf{X}_\alpha^h, t) = \sum_{a \in \check{\mathcal{N}}} N_a^u(\mathbf{X}_\alpha^h) \mathbf{d}_a(t), \quad \Phi^h(\mathbf{X}_\alpha^h, t) = \sum_{b \in \check{\mathcal{M}}} N_b^\Phi(\mathbf{X}_\alpha^h) \phi_b(t) \quad \alpha \in \check{\mathcal{A}} \quad (7)$$

where N_a^u are the shape functions associated with the micromorphic continuum displacement field \mathbf{u}^h , N_b^Φ are the shape functions associated with the micromorphic continuum micro-displacement field Φ^h , and h indicates the characteristic length of the micromorphic FE mesh. Recall that N_a^u and N_b^Φ have compact support and, thus, are only evaluated for DNS nodes that lie within a micromorphic FE containing nodes a and b in its domain.

We now derive the micro-continuum displacement $(\mathbf{u}')^h$ of a micro-element (Fig.3) using the interpolated macro-displacement \mathbf{u}^h and micro-displacement tensor Φ^h in Eq.(7). The position of DNS node α in the current configuration is

$$(\mathbf{x}')^h(\mathbf{X}_\alpha^h, \Xi_\alpha^h, t) = \mathbf{x}^h(\mathbf{X}_\alpha^h, t) + \boldsymbol{\xi}^h(\mathbf{X}_\alpha^h, \Xi_\alpha^h, t) \quad (8)$$

where Ξ_α^h is the reference relative position vector of DNS node α with respect to reference continuum position \mathbf{X}_α^h (e.g., a Gauss point) in \mathcal{B}_0^h , and $\boldsymbol{\xi}^h$ is the current relative position vector of DNS node α with respect to the current continuum position \mathbf{x}^h in \mathcal{B}^h . Introducing the relations,

$$\mathbf{x}^h(\mathbf{X}_\alpha^h, t) = \mathbf{X}_\alpha^h + \mathbf{u}^h(\mathbf{X}_\alpha^h, t) \quad (9)$$

$$\boldsymbol{\xi}^h(\mathbf{X}_\alpha^h, \Xi_\alpha^h, t) = \boldsymbol{\chi}^h(\mathbf{X}_\alpha^h, t) \cdot \Xi_\alpha^h = (\mathbf{1} + \Phi^h(\mathbf{X}_\alpha^h, t)) \cdot \Xi_\alpha^h \quad (10)$$

and substituting into Eq.(8), we have the current position of DNS node α as

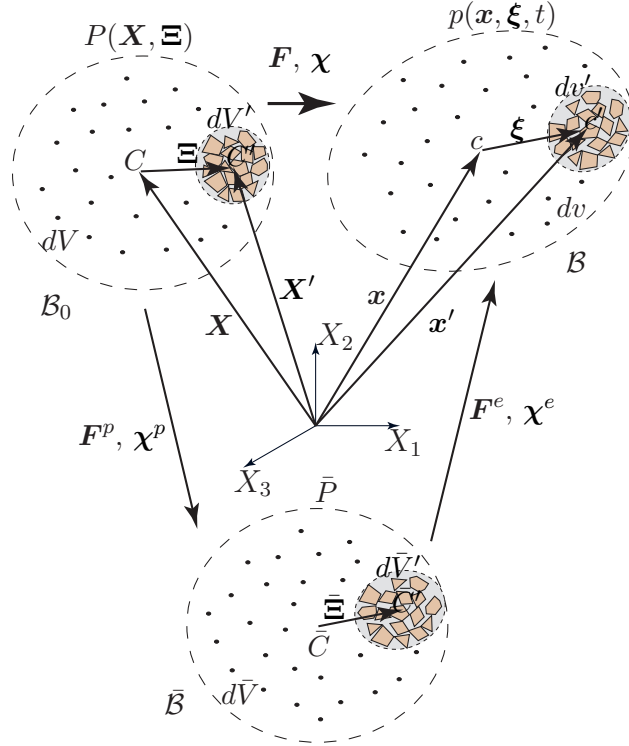


Figure 3. Multiplicative decomposition of deformation gradient \mathbf{F} and micro-deformation tensor χ . Geometrical points (“macro-elements”) with centroids C , \bar{C} , and c live in their respective configurations: $P \in \mathcal{B}_0$, $\bar{P} \in \bar{\mathcal{B}}$, and $p \in \mathcal{B}$. Material points (“micro-elements”) with centroids C' , \bar{C}' , and c' . Differential vectors and deformable directors are mapped accordingly: $d\mathbf{x} = \mathbf{F}d\mathbf{X}$, $d\mathbf{x} = \mathbf{F}^e d\bar{\mathbf{X}}$, $d\bar{\mathbf{X}} = \mathbf{F}^p d\mathbf{X}$, $\xi = \chi \Xi$, $\xi = \chi^e \bar{\Xi}$, and $\bar{\Xi} = \chi^p \Xi$.

$$(\mathbf{x}')^h(\mathbf{X}_\alpha^h, \Xi_\alpha^h, t) = \mathbf{X}_\alpha^h + \mathbf{u}^h(\mathbf{X}_\alpha^h, t) + (\mathbf{1} + \Phi^h(\mathbf{X}_\alpha^h, t)) \cdot \Xi_\alpha^h \quad (11)$$

If we rewrite $(\mathbf{x}')^h$ in terms of its reference position $(\mathbf{X}')^h$, and we introduce a micro-continuum displacement vector $(\mathbf{u}')^h$, we have

$$(\mathbf{x}')^h(\mathbf{X}_\alpha^h, \Xi_\alpha^h, t) = (\mathbf{X}')^h(\mathbf{X}_\alpha^h, \Xi_\alpha^h) + (\mathbf{u}')^h(\mathbf{X}_\alpha^h, \Xi_\alpha^h, t) \quad (12)$$

where $(\mathbf{X}')^h(\mathbf{X}_\alpha^h, \Xi_\alpha^h) = \mathbf{X}_\alpha^h + \Xi_\alpha^h$, then we have

$$(\mathbf{u}')^h(\mathbf{X}_\alpha^h, \Xi_\alpha^h, t) = (\mathbf{x}')^h(\mathbf{X}_\alpha^h, \Xi_\alpha^h, t) - \mathbf{X}_\alpha^h - \Xi_\alpha^h \quad (13)$$

Finally, we have the micro-continuum displacement vector $(\mathbf{u}')^h$ associated with DNS node α , such that

$$\mathbf{q}_\alpha(t) = (\mathbf{u}')^h(\mathbf{X}_\alpha^h, \Xi_\alpha^h, t) = \mathbf{u}^h(\mathbf{X}_\alpha^h, t) + \Phi^h(\mathbf{X}_\alpha^h, t) \cdot \Xi_\alpha^h \quad (14)$$

Then, for all ghost DNS nodes (cf. Fig.2), the interpolations can be written as

$$\hat{\mathbf{Q}} = \mathbf{N}_{\hat{Q}D} \cdot \mathbf{D} + \mathbf{N}_{\hat{Q}\hat{D}} \cdot \hat{\mathbf{D}} \quad (15)$$

where $\mathbf{N}_{\hat{Q}D}$ and $\mathbf{N}_{\hat{Q}\hat{D}}$ are shape function matrices containing individual nodal shape functions N_a^u and N_b^Φ , but for now these matrices will be kept general to increase our flexibility

in choosing interpolation/projection functions (such as those used in meshfree methods). Overall, the DNS nodal displacements may be written as

$$\begin{bmatrix} \mathbf{Q} \\ \widehat{\mathbf{Q}} \end{bmatrix} = \begin{bmatrix} \mathbf{N}_{QD} & \mathbf{N}_{Q\widehat{D}} \\ \mathbf{N}_{\widehat{Q}D} & \mathbf{N}_{\widehat{Q}\widehat{D}} \end{bmatrix} \cdot \begin{bmatrix} \mathbf{D} \\ \widehat{\mathbf{D}} \end{bmatrix} + \begin{bmatrix} \mathbf{Q}' \\ \mathbf{0} \end{bmatrix} \quad (16)$$

where \mathbf{Q}' is introduced [Klein and Zimmerman, 2006] as the error (or “fine-scale” [Wagner and Liu, 2003]) in the interpolation of the free DNS nodal displacements \mathbf{Q} , whose function space is not rich enough to represent the true free DNS motion. The shape function matrices \mathbf{N} are, in general, not square because the number of free DNS dofs are not the same as free and prescribed micromorphic FE dofs, and the number of ghost DNS dofs is not the same as prescribed and free micromorphic FE dofs. A scalar measure of error e in DNS nodal displacements is defined as [Klein and Zimmerman, 2006]

$$e = \mathbf{Q}' \cdot \mathbf{Q}' \quad (17)$$

which may be minimized with respect to prescribed micromorphic continuum FE nodal dofs $\widehat{\mathbf{D}}$ to solve for $\widehat{\mathbf{D}}$ in terms of free DNS dofs and micromorphic continuum FE nodal dofs as

$$\widehat{\mathbf{D}} = \mathbf{M}_{\widehat{D}\widehat{D}}^{-1} \mathbf{N}_{Q\widehat{D}}^T (\mathbf{Q} - \mathbf{N}_{QD} \mathbf{D}), \quad \mathbf{M}_{\widehat{D}\widehat{D}} = \mathbf{N}_{Q\widehat{D}}^T \mathbf{N}_{Q\widehat{D}} \quad (18)$$

This is known as the “discretized L_2 projection” [Klein and Zimmerman, 2006] of the free DNS nodal dofs \mathbf{Q} and free micromorphic FE nodal dofs \mathbf{D} onto the prescribed micromorphic FE nodal dofs $\widehat{\mathbf{D}}$. Upon substituting Eq.(18) into Eq.(15), we may write the prescribed DNS dofs $\widehat{\mathbf{Q}}$ in terms of free DNS dofs \mathbf{Q} and micromorphic continuum FE nodal dofs \mathbf{D} . In summary, these relations are written as

$$\widehat{\mathbf{Q}} = \mathbf{B}_{\widehat{Q}Q} \mathbf{Q} + \mathbf{B}_{\widehat{Q}D} \mathbf{D} \quad (19)$$

$$\widehat{\mathbf{D}} = \mathbf{B}_{\widehat{D}Q} \mathbf{Q} + \mathbf{B}_{\widehat{D}D} \mathbf{D} \quad (20)$$

where

$$\mathbf{B}_{\widehat{Q}Q} = \mathbf{N}_{\widehat{Q}\widehat{D}} \mathbf{B}_{\widehat{D}Q} \quad (21)$$

$$\mathbf{B}_{\widehat{Q}D} = \mathbf{N}_{\widehat{Q}D} + \mathbf{N}_{\widehat{Q}\widehat{D}} \mathbf{B}_{\widehat{D}D} \quad (22)$$

$$\mathbf{B}_{\widehat{D}Q} = \mathbf{M}_{\widehat{D}\widehat{D}}^{-1} \mathbf{N}_{Q\widehat{D}}^T \quad (23)$$

$$\mathbf{B}_{\widehat{D}D} = -\mathbf{M}_{\widehat{D}\widehat{D}}^{-1} \mathbf{N}_{Q\widehat{D}}^T \mathbf{N}_{QD} \quad (24)$$

As shown in Fig.2, for a finite element implementation of this dof coupling, we expect that free DNS dofs \mathbf{Q} will not fall within the support of free micromorphic continuum FE nodal dofs \mathbf{D} , such that it can be assumed that $\mathbf{N}_{QD} = \mathbf{0}$ and

$$\widehat{\mathbf{Q}} = \mathbf{B}_{\widehat{Q}Q} \mathbf{Q} + \mathbf{B}_{\widehat{Q}D} \mathbf{D}, \quad \widehat{\mathbf{D}} = \mathbf{B}_{\widehat{D}Q} \mathbf{Q} \quad (25)$$

where

$$\mathbf{B}_{\widehat{Q}Q} = \mathbf{N}_{\widehat{Q}\widehat{D}} \mathbf{B}_{\widehat{D}Q}, \quad \mathbf{B}_{\widehat{Q}D} = \mathbf{N}_{\widehat{Q}D} \quad (26)$$

$$\mathbf{B}_{\widehat{D}Q} = \mathbf{M}_{\widehat{D}\widehat{D}}^{-1} \mathbf{N}_{Q\widehat{D}}^T, \quad \mathbf{B}_{\widehat{D}D} = \mathbf{0} \quad (27)$$

The assumption $\mathbf{N}_{QD} \neq \mathbf{0}$ would be valid for a meshfree projection of the DNS nodal dofs to the micromorphic FE nodal dofs, as in Klein and Zimmerman [2006], where we could

imagine that the domain of influence of the meshfree projection could encompass a free DNS node; the degree of encompassment would be controlled by the chosen support size of the meshfree kernel function. The choice of meshfree projection in Klein and Zimmerman [2006] was not necessarily to allow \mathbf{Q} be projected to \mathbf{D} (and vice versa), but to remove the computationally costly calculation of the inverse $\mathbf{M}_{\hat{D}\hat{D}}^{-1}$ in Eqs. (19) and (20).

3.1.2 3D Kinetic and Potential Energy Partitioning and Coupling

For the DNS equations, the kinetic energy is T^Q , dissipation function F^Q , and potential energy U^Q , such that

$$\begin{aligned} T^Q &= \frac{1}{2} \dot{\mathbf{Q}} \mathbf{M}^Q \dot{\mathbf{Q}} \\ F^Q &= a_Q T^Q \\ U^Q(\mathbf{Q}) &= \int_{\mathbf{0}}^{\mathbf{Q}} \mathbf{F}^{INT,Q}(\mathbf{S}) d\mathbf{S} \end{aligned} \quad (28)$$

where \mathbf{M}^Q is the mass matrix, and $\mathbf{F}^{INT,Q}$ is an internal force vector for the DNS region. The dissipation function F^Q is written as a linear function of the kinetic energy T^Q with proportionality coefficient a_Q , which falls within the class of damping called ‘‘Rayleigh damping’’ (pg.130 of Rayleigh [1945]). For the micromorphic continuum FE equations, T^D is the kinetic energy, F^D the dissipation function, and U^D the potential energy, such that

$$\begin{aligned} T^D &= \frac{1}{2} \dot{\mathbf{D}} \mathbf{M}^D \dot{\mathbf{D}} \\ F^D &= a_D T^D \\ U^D(\mathbf{D}) &= \int_{\mathbf{0}}^{\mathbf{D}} \mathbf{F}^{INT,D}(\mathbf{S}) d\mathbf{S} \end{aligned} \quad (29)$$

where \mathbf{M}^D is the mass and micro-inertia matrix, and $\mathbf{F}^{INT,D}$ is the internal force vector. We assume the total kinetic and potential energy and dissipation of the coupled DNS-micromorphic-continuum system may be written as the sum of the energies

$$T(\dot{\mathbf{Q}}, \dot{\mathbf{D}}) = T^Q(\dot{\mathbf{Q}}, \hat{\mathbf{Q}}(\dot{\mathbf{Q}}, \dot{\mathbf{D}})) + T^D(\dot{\mathbf{D}}, \hat{\mathbf{D}}(\dot{\mathbf{Q}})) \quad (30)$$

$$U(\mathbf{Q}, \mathbf{D}) = U^Q(\mathbf{Q}, \hat{\mathbf{Q}}(\mathbf{Q}, \mathbf{D})) + U^D(\mathbf{D}, \hat{\mathbf{D}}(\mathbf{Q})) \quad (31)$$

$$F(\dot{\mathbf{Q}}, \dot{\mathbf{D}}) = F^Q(\dot{\mathbf{Q}}, \hat{\mathbf{Q}}(\dot{\mathbf{Q}}, \dot{\mathbf{D}})) + F^D(\dot{\mathbf{D}}, \hat{\mathbf{D}}(\dot{\mathbf{Q}})) \quad (32)$$

where we have indicated the functional dependence of the prescribed DNS dofs and micromorphic FE dofs solely upon the free DNS dofs and micromorphic FE dofs \mathbf{Q} and \mathbf{D} , respectively. Lagrange’s equations may then be stated as

$$\begin{aligned} \frac{d}{dt} \left(\frac{\partial T}{\partial \dot{\mathbf{Q}}} \right) - \frac{\partial T}{\partial \mathbf{Q}} + \frac{\partial F}{\partial \dot{\mathbf{Q}}} + \frac{\partial U}{\partial \mathbf{Q}} &= \mathbf{F}^{EXT,Q} \\ \frac{d}{dt} \left(\frac{\partial T}{\partial \dot{\mathbf{D}}} \right) - \frac{\partial T}{\partial \mathbf{D}} + \frac{\partial F}{\partial \dot{\mathbf{D}}} + \frac{\partial U}{\partial \mathbf{D}} &= \mathbf{F}^{EXT,D} \end{aligned} \quad (33)$$

which lead to a coupled system of governing equations (linear and first moment of momentum) for the coupled DNS-micromorphic-continuum mechanics. The derivatives are

$$\frac{\partial T}{\partial \dot{\mathbf{Q}}} = \frac{\partial T^Q}{\partial \dot{\mathbf{Q}}} + \frac{\partial T^Q}{\partial \dot{\hat{\mathbf{Q}}}} \mathbf{B}_{\hat{\mathbf{Q}}Q} + \frac{\partial T^D}{\partial \dot{\hat{\mathbf{D}}}} \mathbf{B}_{\hat{\mathbf{D}}Q}, \quad \frac{\partial T}{\partial \mathbf{Q}} = \mathbf{0} \quad (34)$$

$$\frac{\partial F}{\partial \dot{\mathbf{Q}}} = \frac{\partial F^Q}{\partial \dot{\mathbf{Q}}} + \frac{\partial F^D}{\partial \dot{\hat{\mathbf{Q}}}} = a_Q \left(\frac{\partial T^Q}{\partial \dot{\mathbf{Q}}} + \frac{\partial T^Q}{\partial \dot{\hat{\mathbf{Q}}}} \mathbf{B}_{\hat{\mathbf{Q}}Q} \right) + a_D \left(\frac{\partial T^D}{\partial \dot{\hat{\mathbf{D}}}} \mathbf{B}_{\hat{\mathbf{D}}Q} \right) \quad (35)$$

$$\frac{\partial U}{\partial \mathbf{Q}} = \frac{\partial U^Q}{\partial \mathbf{Q}} + \frac{\partial U^Q}{\partial \hat{\mathbf{Q}}} \mathbf{B}_{\hat{\mathbf{Q}}Q} + \frac{\partial U^D}{\partial \hat{\mathbf{D}}} \mathbf{B}_{\hat{\mathbf{D}}Q} \quad (36)$$

$$\frac{\partial T}{\partial \dot{\hat{\mathbf{D}}}} = \frac{\partial T^D}{\partial \dot{\hat{\mathbf{D}}}} + \frac{\partial T^D}{\partial \dot{\hat{\mathbf{Q}}}} \mathbf{B}_{\hat{\mathbf{D}}D} + \frac{\partial T^Q}{\partial \dot{\hat{\mathbf{Q}}}} \mathbf{B}_{\hat{\mathbf{Q}}D}, \quad \frac{\partial T}{\partial \mathbf{D}} = \mathbf{0} \quad (37)$$

$$\frac{\partial F}{\partial \dot{\hat{\mathbf{D}}}} = \frac{\partial F^Q}{\partial \dot{\hat{\mathbf{D}}}} + \frac{\partial F^D}{\partial \dot{\hat{\mathbf{D}}}} = a_Q \left(\frac{\partial T^Q}{\partial \dot{\hat{\mathbf{Q}}}} \mathbf{B}_{\hat{\mathbf{Q}}D} \right) + a_D \left(\frac{\partial T^D}{\partial \dot{\hat{\mathbf{D}}}} \right) \quad (38)$$

$$\frac{\partial U}{\partial \mathbf{D}} = \frac{\partial U^D}{\partial \mathbf{D}} + \frac{\partial U^D}{\partial \hat{\mathbf{D}}} \mathbf{B}_{\hat{\mathbf{D}}D} + \frac{\partial U^Q}{\partial \hat{\mathbf{Q}}} \mathbf{B}_{\hat{\mathbf{Q}}D} \quad (39)$$

If the potential energy U is nonlinear with regard to DNS constitutive models and micromorphic elasto-plasticity, then Eq.(33) may be integrated in time and linearized for solution by the Newton-Raphson method. The benefit of this multiscale method, as pointed out by Wagner and Liu [2003], is that time steps may be different for the DNS and micromorphic FE solutions. A multiscale time stepping scheme will follow an approach similar to Wagner and Liu [2003]. To complete Eq.(33) and identify an approach to energy partitioning, the individual derivatives may be written as

$$\frac{\partial T^Q}{\partial \dot{\mathbf{Q}}} = \mathbf{M}^Q \dot{\mathbf{Q}}, \quad \frac{\partial T^Q}{\partial \dot{\hat{\mathbf{Q}}}} = \mathbf{M}^{\hat{\mathbf{Q}}} \dot{\hat{\mathbf{Q}}} \quad (40)$$

$$\frac{\partial T^D}{\partial \dot{\hat{\mathbf{D}}}} = \mathbf{M}^D \dot{\hat{\mathbf{D}}}, \quad \frac{\partial T^D}{\partial \dot{\hat{\mathbf{Q}}}} = \mathbf{M}^{\hat{\mathbf{D}}} \dot{\hat{\mathbf{D}}} \quad (41)$$

$$\frac{\partial F}{\partial \dot{\mathbf{Q}}} = a_Q \left(\mathbf{M}^Q \dot{\mathbf{Q}} + \mathbf{B}_{\hat{\mathbf{Q}}Q}^T \mathbf{M}^{\hat{\mathbf{Q}}} \dot{\hat{\mathbf{Q}}} \right) + a_D \left(\mathbf{B}_{\hat{\mathbf{D}}Q}^T \mathbf{M}^{\hat{\mathbf{D}}} \dot{\hat{\mathbf{D}}} \right) \quad (42)$$

$$\frac{\partial F}{\partial \dot{\hat{\mathbf{D}}}} = a_Q \left(\mathbf{B}_{\hat{\mathbf{Q}}D}^T \mathbf{M}^{\hat{\mathbf{Q}}} \dot{\hat{\mathbf{Q}}} \right) + a_D \left(\mathbf{M}^D \dot{\hat{\mathbf{D}}} \right) \quad (43)$$

$$\frac{\partial U^Q}{\partial \mathbf{Q}} = \mathbf{F}^{INT,Q}(\mathbf{Q}), \quad \frac{\partial U^Q}{\partial \hat{\mathbf{Q}}} = \mathbf{F}^{INT,\hat{\mathbf{Q}}}(\hat{\mathbf{Q}}) \quad (44)$$

$$\frac{\partial U^D}{\partial \mathbf{D}} = \mathbf{F}^{INT,D}(\mathbf{D}), \quad \frac{\partial U^D}{\partial \hat{\mathbf{D}}} = \mathbf{F}^{INT,\hat{\mathbf{D}}}(\hat{\mathbf{D}}) \quad (45)$$

where superscript Q denotes free DNS dofs and \hat{Q} ghost DNS dofs, whereas superscript D denotes free micromorphic FE dofs and \hat{D} prescribed micromorphic FE dofs. The energy partitioning will be introduced through the definition of these terms below. First, substitute Eqs. (40)–(45) into Eq.(33) to arrive at the coupled nonlinear equations in terms of \mathbf{Q} and \mathbf{D} as

$$\begin{aligned}
& \left(\mathbf{M}^Q + \mathbf{B}_{\hat{Q}Q}^T \mathbf{M}^{\hat{Q}} \mathbf{B}_{\hat{Q}Q} + \mathbf{B}_{\hat{D}Q}^T \mathbf{M}^{\hat{D}} \mathbf{B}_{\hat{D}Q} \right) \ddot{\mathbf{Q}} \\
& + \left(\mathbf{B}_{\hat{Q}Q}^T \mathbf{M}^{\hat{Q}} \mathbf{B}_{\hat{Q}D} + \mathbf{B}_{\hat{D}Q}^T \mathbf{M}^{\hat{D}} \mathbf{B}_{\hat{D}D} \right) \ddot{\mathbf{D}} \\
& + \left(a_Q \mathbf{M}^Q + a_Q \mathbf{B}_{\hat{Q}Q}^T \mathbf{M}^{\hat{Q}} \mathbf{B}_{\hat{Q}Q} + a_D \mathbf{B}_{\hat{D}Q}^T \mathbf{M}^{\hat{D}} \mathbf{B}_{\hat{D}Q} \right) \dot{\mathbf{Q}} + a_Q \mathbf{B}_{\hat{Q}Q}^T \mathbf{M}^{\hat{Q}} \mathbf{B}_{\hat{Q}D} \dot{\mathbf{D}} \\
& + \mathbf{F}^{INT,Q}(\mathbf{Q}) + \mathbf{B}_{\hat{Q}Q}^T \mathbf{F}^{INT,\hat{Q}}[\mathbf{B}_{\hat{Q}Q} \mathbf{Q} + \mathbf{B}_{\hat{Q}D} \mathbf{D}] \\
& + \mathbf{B}_{\hat{D}Q}^T \mathbf{F}^{INT,\hat{D}}[\mathbf{B}_{\hat{D}Q} \mathbf{Q} + \mathbf{B}_{\hat{D}D} \mathbf{D}] = \mathbf{F}^{EXT,Q} + \mathbf{B}_{\hat{Q}Q}^T \mathbf{F}^{EXT,\hat{Q}}
\end{aligned} \tag{46}$$

$$\begin{aligned}
& \left(\mathbf{B}_{\hat{Q}D}^T \mathbf{M}^{\hat{Q}} \mathbf{B}_{\hat{Q}D} + \mathbf{B}_{\hat{D}D}^T \mathbf{M}^{\hat{D}} \mathbf{B}_{\hat{D}D} \right) \ddot{\mathbf{Q}} \\
& + \left(\mathbf{M}^D + \mathbf{B}_{\hat{Q}D}^T \mathbf{M}^{\hat{Q}} \mathbf{B}_{\hat{Q}D} + \mathbf{B}_{\hat{D}D}^T \mathbf{M}^{\hat{D}} \mathbf{B}_{\hat{D}D} \right) \ddot{\mathbf{D}} \\
& + a_Q \mathbf{B}_{\hat{Q}D}^T \mathbf{M}^{\hat{Q}} \mathbf{B}_{\hat{Q}Q} \dot{\mathbf{Q}} + \left(a_Q \mathbf{B}_{\hat{Q}D}^T \mathbf{M}^{\hat{Q}} \mathbf{B}_{\hat{Q}D} + a_D \mathbf{M}^D \right) \dot{\mathbf{D}} \\
& + \mathbf{B}_{\hat{Q}D}^T \mathbf{F}^{INT,\hat{Q}}[\mathbf{B}_{\hat{Q}Q} \mathbf{Q} + \mathbf{B}_{\hat{Q}D} \mathbf{D}] + \mathbf{B}_{\hat{D}D}^T \mathbf{F}^{INT,\hat{D}}[\mathbf{B}_{\hat{D}Q} \mathbf{Q} + \mathbf{B}_{\hat{D}D} \mathbf{D}] \\
& + \mathbf{F}^{INT,D}(\mathbf{D}) = \mathbf{F}^{EXT,D} + \mathbf{B}_{\hat{D}D}^T \mathbf{F}^{EXT,\hat{D}}
\end{aligned} \tag{47}$$

where an expression in brackets $[\bullet]$ denotes the functional dependence of the nonlinear internal force vector. Note the projections through the \mathbf{B} matrices of the corresponding mass and damping matrices, and forcing vectors. First, starting with the mass matrices for the DNS nodes, we partition the kinetic energy (and, in turn, the dissipation functions) as follows:

$$\mathbf{M}^{\hat{Q}} = (1 - \hat{r}) \mathbf{A} \underset{\alpha}{m}_{\alpha}^Q, \quad \alpha \in \hat{\mathcal{A}}, \quad \mathbf{x}_{\alpha} \in \tilde{\mathcal{B}}^h \tag{48}$$

$$\mathbf{M}^Q = \mathbf{M}^{DNS,Q} + \widehat{\mathbf{M}}^Q \tag{49}$$

$$\mathbf{M}^{DNS,Q} = \mathbf{A} \underset{\beta}{m}_{\beta}^Q, \quad \beta \in \mathcal{A}, \quad \mathbf{x}_{\beta} \in \mathcal{B}^{DNS}$$

$$\widehat{\mathbf{M}}^Q = (1 - \hat{r}) \mathbf{A} \underset{\beta}{m}_{\beta}^Q, \quad \beta \in \mathcal{A}, \quad \mathbf{x}_{\beta} \in \hat{\mathcal{B}}^h$$

where $\mathbf{M}^{\hat{Q}}$ is the mass matrix of ghost DNS nodes in $\tilde{\mathcal{B}}^h$, $\mathbf{M}^{DNS,Q}$ the mass matrix of free DNS nodes in \mathcal{B}^{DNS} , $\widehat{\mathbf{M}}^Q$ the mass matrix of free DNS nodes in $\hat{\mathcal{B}}^h$, and \hat{r} is a weighting factor for the kinetic energy in the overlap region $\hat{\mathcal{B}}^h \cup \tilde{\mathcal{B}}^h$. For no homogenized micromorphic continuum contribution to the kinetic energy in the overlap region, $\hat{r} = 0$, and for full micromorphic continuum homogenization of the underlying DNS kinetic energy, $\hat{r} = 1$. In our case, we will consider the range $0 \leq \hat{r} \leq 1$. Given that the proposed multiscale modeling framework is to be used in an adaptive fashion in the future, having an overlaying micromorphic continuum homogenization of the DNS response is attractive when DNS is converted to micromorphic continuum representation, and vice versa (in a statistical manner*). For the

*statistical, in the sense of generating a DNS representation from a micromorphic continuum one, where the underlying DNS region does not exist; converting from DNS to micromorphic continuum representation is straightforward given the built-in homogenization that the micromorphic continuum possesses

mass and micro-inertia matrices associated with the micromorphic continuum, we partition the kinetic energy as follows:

$$\begin{aligned}
\mathbf{M}^{\hat{D}} &= \widetilde{\mathbf{M}}^{\hat{D}} + \widehat{\mathbf{M}}^{\hat{D}} & (50) \\
\widetilde{\mathbf{M}}^{\check{D}} &= \begin{bmatrix} \widetilde{\mathbf{M}}^{\check{u}} & \mathbf{0} \\ \mathbf{0} & \widetilde{\mathbf{M}}^{\check{\Phi}} \end{bmatrix} \\
\widetilde{\mathbf{M}}^{\check{u}} &= \mathbf{A} \left(\hat{r} \langle \mathbf{m}^{u,e} \rangle + \tilde{r}^e \mathbf{m}^{u,e} \right) \\
\widetilde{\mathbf{M}}^{\check{\Phi}} &= \mathbf{A} \left(\hat{r} \langle \mathbf{m}^{\Phi,e} \rangle + \tilde{r}^e \mathbf{m}^{\Phi,e} \right) \\
\widehat{\mathbf{M}}^{\hat{D}} &= \hat{r} \begin{bmatrix} \widehat{\mathbf{M}}^{\hat{u}} & \mathbf{0} \\ \mathbf{0} & \widehat{\mathbf{M}}^{\hat{\Phi}} \end{bmatrix}, \quad \widehat{\mathbf{M}}^{\hat{u}} = \mathbf{A} \langle \mathbf{m}^{u,e} \rangle, \quad \widehat{\mathbf{M}}^{\hat{\Phi}} = \mathbf{A} \langle \mathbf{m}^{\Phi,e} \rangle \\
\mathbf{M}^D &= \widetilde{\mathbf{M}}^D + \bar{\mathbf{M}}^D & (51) \\
\bar{\mathbf{M}}^D &= \begin{bmatrix} \bar{\mathbf{M}}^u & \mathbf{0} \\ \mathbf{0} & \bar{\mathbf{M}}^{\Phi} \end{bmatrix}, \quad \bar{\mathbf{M}}^u = \mathbf{A} \mathbf{m}^{u,e}, \quad \bar{\mathbf{M}}^{\Phi} = \mathbf{A} \mathbf{m}^{\Phi,e}
\end{aligned}$$

where $\widetilde{\mathbf{M}}^{\hat{D}}$ is the micromorphic continuum mass and micro-inertia matrix associated with prescribed micromorphic FE dofs in $\tilde{\mathcal{B}}^h$, $\widetilde{\mathbf{M}}^D$ the micromorphic continuum mass and micro-inertia matrix associated with free micromorphic FE dofs in $\tilde{\mathcal{B}}^h$, where $\widetilde{\mathbf{M}}^{\hat{D}}$ and $\widetilde{\mathbf{M}}^D$ are extracted from the total mass and micro-inertia matrix $\widetilde{\mathbf{M}}^{\check{D}}$ in $\tilde{\mathcal{B}}^h$, with superscript $(\bullet)^{\check{D}}$ denoting the full mass and micro-inertia matrix associated with elements in $\tilde{\mathcal{B}}^h$, $\langle \bullet \rangle$ is a homogenization operator, \tilde{r}^e is the partitioning coefficient of micromorphic continuum kinetic energy associated with element $\mathcal{B}^e \subset \tilde{\mathcal{B}}^h$. A simple choice is a volume fraction $\tilde{r}^e = \mathcal{B}^{e,D} / \mathcal{B}^e$, where $\mathcal{B}^{e,D} = \mathcal{B}^e - \mathcal{B}^{e,\hat{Q}}$; $\mathcal{B}^{e,D}$ is the non-overlapping micromorphic continuum part of element volume $\mathcal{B}^e \subset \tilde{\mathcal{B}}^h$, and $\mathcal{B}^{e,\hat{Q}}$ is the overlapped ghost DNS volume in the element (cf. Fig.2). For kinetic energy partitioning, a volume fraction that directly relates to mass and micro-inertia partitioning seems an appropriate choice. $\widehat{\mathbf{M}}^{\hat{D}}$ is the homogenized micromorphic continuum mass and micro-inertia matrix associated with prescribed micromorphic FE dofs in $\hat{\mathcal{B}}^h$; where if $\hat{r} = 0$, there is no micromorphic continuum homogenization in $\hat{\mathcal{B}}^h$ (i.e., all kinetic energy is due to underlying DNS). $\bar{\mathbf{M}}^D$ is the micromorphic continuum mass and micro-inertia matrix associated with free micromorphic FE nodal dofs in the pure micromorphic continuum FE domain $\bar{\mathcal{B}}^h$.

For the potential energy (internal force) and external force partitioning in the DNS system, we write

$$\mathbf{F}^{INT,\hat{Q}} = (1 - \hat{q}) \mathbf{A} \underset{\epsilon}{f}^{\epsilon INT,Q}, \mathbf{x}_\epsilon \in \tilde{\mathcal{B}}^h \quad (52)$$

$$\mathbf{F}^{INT,Q} = \mathbf{F}^{INT,DNS,Q} + \hat{\mathbf{F}}^{INT,Q} \quad (53)$$

$$\mathbf{F}^{INT,DNS,Q} = \mathbf{A} \underset{\delta}{f}^{\delta INT,Q}, \mathbf{x}_\delta \in \mathcal{B}^{DNS}$$

$$\hat{\mathbf{F}}^{INT,Q} = (1 - \hat{q}) \mathbf{A} \underset{\delta}{f}^{\delta INT,Q}, \mathbf{x}_\delta \in \hat{\mathcal{B}}^h$$

$$\mathbf{F}^{EXT,\hat{Q}} = (1 - \hat{q}) \mathbf{A} \underset{\epsilon}{f}^{\epsilon EXT,Q}, \mathbf{x}_\epsilon \in \tilde{\mathcal{B}}^h \quad (54)$$

$$\mathbf{F}^{EXT,Q} = \mathbf{F}^{EXT,DNS,Q} + \hat{\mathbf{F}}^{EXT,Q} \quad (55)$$

$$\mathbf{F}^{EXT,DNS,Q} = \mathbf{A} \underset{\delta}{f}^{\delta EXT,Q}, \mathbf{x}_\delta \in \mathcal{B}^{DNS}$$

$$\hat{\mathbf{F}}^{EXT,Q} = (1 - \hat{q}) \mathbf{A} \underset{\delta}{f}^{\delta EXT,Q}, \mathbf{x}_\delta \in \hat{\mathcal{B}}^h$$

where $\mathbf{F}^{INT,\hat{Q}}$ is the internal force vector associated with ghost DNS nodes in $\tilde{\mathcal{B}}^h$, $\mathbf{F}^{INT,DNS,Q}$ is the internal force vector associated with free DNS nodes in \mathcal{B}^{DNS} , $\hat{\mathbf{F}}^{INT,Q}$ is the internal force vector associated with free DNS nodes in $\hat{\mathcal{B}}^h$, $\mathbf{F}^{EXT,\hat{Q}}$ is the external force vector associated with ghost DNS nodes in $\tilde{\mathcal{B}}^h$, $\mathbf{F}^{EXT,DNS,Q}$ is the external force vector associated with free DNS nodes in \mathcal{B}^{DNS} , $\hat{\mathbf{F}}^{EXT,Q}$ is the external force vector associated with free DNS nodes in $\hat{\mathcal{B}}^h$, and \hat{q} is a weighting factor for the potential energy in the overlap region $\tilde{\mathcal{B}}^h \cup \hat{\mathcal{B}}^h$. For no homogenized micromorphic continuum contribution to the potential energy in the overlap region, $\hat{q} = 0$, and for full micromorphic continuum homogenization of the underlying DNS potential energy, $\hat{q} = 1$. In our case, we will consider the range $0 \leq \hat{q} \leq 1$. Note that in Klein and Zimmerman [2006], they chose $\hat{q} = 0$. Their Cauchy-Born elastic constitutive model acts like a homogenization operator on the underlying atomistic response, but instead of keeping an overlain Cauchy-Born representation, the potential energy is completely represented by the underlying atomistic response, except in the overlap region $\tilde{\mathcal{B}}^h$ where partitioning occurs. Note that \mathbf{x}_ϵ and \mathbf{x}_δ denote positions of DNS nodes for calculating internal force vectors in Eqs. (52)–(56), whereas \mathbf{x}_α and \mathbf{x}_β in Eqs. (48) and (49) denote DNS nodes for calculating DNS mass matrices.

For the potential energy (internal force) partitioning in the micromorphic continuum, we write

$$\mathbf{F}^{INT,D} = \tilde{\mathbf{F}}^{INT,D} + \bar{\mathbf{F}}^{INT,D} \quad (56)$$

$$\bar{\mathbf{F}}^{INT,D} = \begin{bmatrix} \bar{\mathbf{F}}^{INT,u} \\ \bar{\mathbf{F}}^{INT,\Phi} \end{bmatrix}$$

$$\bar{\mathbf{F}}^{INT,u} = \mathbf{A} \underset{e \in \tilde{\mathcal{B}}^h}{f}^{INT,u,e}, \quad \bar{\mathbf{F}}^{INT,\Phi} = \mathbf{A} \underset{e \in \tilde{\mathcal{B}}^h}{f}^{INT,\Phi,e}$$

and

$$\begin{aligned}
\mathbf{F}^{INT,\hat{D}} &= \tilde{\mathbf{F}}^{INT,\hat{D}} + \hat{\mathbf{F}}^{INT,\hat{D}} \\
\tilde{\mathbf{F}}^{INT,\hat{D}} &= \begin{bmatrix} \tilde{\mathbf{F}}^{INT,\hat{u}} \\ \tilde{\mathbf{F}}^{INT,\hat{\Phi}} \end{bmatrix} \\
\tilde{\mathbf{F}}^{INT,\hat{u}} &= \mathbf{A} \left(\hat{q} \langle \mathbf{f}^{INT,u,e} \rangle + \tilde{q}^e \mathbf{f}^{INT,u,e} \right) \\
\langle \mathbf{f}^{INT,u,e} \rangle &= \int_{\mathcal{B}^e} (\mathbf{B}^{u,e})^T \cdot \langle \boldsymbol{\sigma} \rangle dv \\
\tilde{\mathbf{F}}^{INT,\hat{\Phi}} &= \mathbf{A} \left(\hat{q} \langle \mathbf{f}^{INT,\Phi,e} \rangle + \tilde{q}^e \mathbf{f}^{INT,\Phi,e} \right) \\
\hat{\mathbf{F}}^{INT,\hat{D}} &= \hat{q} \begin{bmatrix} \hat{\mathbf{F}}^{INT,\hat{u}} \\ \hat{\mathbf{F}}^{INT,\hat{\Phi}} \end{bmatrix} \\
\hat{\mathbf{F}}^{INT,\hat{u}} &= \mathbf{A} \langle \mathbf{f}^{INT,u,e} \rangle, \quad \hat{\mathbf{F}}^{INT,\hat{\Phi}} = \mathbf{A} \langle \mathbf{f}^{INT,\Phi,e} \rangle
\end{aligned} \tag{57}$$

where $\tilde{\mathbf{F}}^{INT,D}$ is the internal force vector associated with free micromorphic FE dofs in $\tilde{\mathcal{B}}^h$, $\tilde{\mathbf{F}}^{INT,\hat{D}}$ the internal force vector associated with prescribed micromorphic FE dofs in $\tilde{\mathcal{B}}^h$, where $\tilde{\mathbf{F}}^{INT,D}$ and $\tilde{\mathbf{F}}^{INT,\hat{D}}$ are extracted from the full internal force vector $\tilde{\mathbf{F}}^{INT,\hat{D}}$, with superscript $(\bullet)^{\hat{D}}$ denoting the full internal force vector associated with elements in $\tilde{\mathcal{B}}^h$, \tilde{q}^e is the partitioning coefficient of micromorphic continuum potential energy associated with element $\mathcal{B}^e \subset \tilde{\mathcal{B}}^h$, and $\langle \bullet \rangle$ is a homogenization operator (to be defined later). A simple choice is a volume fraction $\tilde{q}^e = \tilde{r}^e$. Klein and Zimmerman [2006] considered a more sophisticated approach using an atomic bond density function solved to reproduce a minimum potential energy state for homogeneous deformation. The analogy here for DNS nodes would be a DNS potential energy term (internal force vectors). This will be considered further in future work. For now, we consider a volume fraction partitioning through \tilde{q}^e , and a simple scaling through coefficients \hat{q} . $\hat{\mathbf{F}}^{INT,\hat{D}}$ is the homogenized internal force vector associated with prescribed micromorphic FE dofs in $\hat{\mathcal{B}}^h$, which has no contribution if $\hat{q} = 0$, i.e., underlying DNS internal forces provide full contribution in $\hat{\mathcal{B}}^h$. $\bar{\mathbf{F}}^{INT,D}$ is the internal force vector associated with free micromorphic FE dofs in the pure micromorphic continuum domain $\bar{\mathcal{B}}^h$. The external force vector is written as

$$\begin{aligned}
\mathbf{F}^{EXT,D} &= \tilde{\mathbf{F}}^{EXT,D} + \bar{\mathbf{F}}^{EXT,D} \\
\bar{\mathbf{F}}^{EXT,D} &= \begin{bmatrix} \bar{\mathbf{F}}^{EXT,u} \\ \bar{\mathbf{F}}^{EXT,\Phi} \end{bmatrix} \\
\bar{\mathbf{F}}^{EXT,u} &= \mathbf{F}_t + \mathbf{F}_g + \mathbf{A} \mathbf{f}_b^{EXT,u,e} \\
\bar{\mathbf{F}}^{EXT,\Phi} &= \mathbf{F}_r + \mathbf{F}_g^\Phi + \mathbf{A} \mathbf{f}_\ell^{EXT,\Phi,e}
\end{aligned} \tag{58}$$

and

$$\begin{aligned}
\mathbf{F}^{EXT,\hat{D}} &= \tilde{\mathbf{F}}^{EXT,\hat{D}} + \hat{\mathbf{F}}^{EXT,\hat{D}} \\
\tilde{\mathbf{F}}^{EXT,\check{D}} &= \begin{bmatrix} \tilde{\mathbf{F}}^{EXT,\check{u}} \\ \tilde{\mathbf{F}}^{EXT,\check{\Phi}} \end{bmatrix} \\
\tilde{\mathbf{F}}^{EXT,\check{u}} &= \mathbf{A} \left(\hat{q} \left\langle \mathbf{f}_b^{EXT,u,e} \right\rangle + \tilde{q}^e \mathbf{f}_b^{EXT,u,e} \right) \\
\tilde{\mathbf{F}}^{EXT,\check{\Phi}} &= \mathbf{A} \left(\hat{q} \left\langle \mathbf{f}_\ell^{EXT,\Phi,e} \right\rangle + \tilde{q}^e \mathbf{f}_\ell^{EXT,\Phi,e} \right) \\
\hat{\mathbf{F}}^{EXT,\hat{D}} &= \hat{q} \begin{bmatrix} \hat{\mathbf{F}}^{EXT,\hat{u}} \\ \hat{\mathbf{F}}^{EXT,\hat{\Phi}} \end{bmatrix} \\
\hat{\mathbf{F}}^{EXT,\hat{u}} &= \mathbf{A} \left\langle \mathbf{f}_b^{EXT,u,e} \right\rangle, \quad \hat{\mathbf{F}}^{EXT,\hat{\Phi}} = \mathbf{A} \left\langle \mathbf{f}_\ell^{EXT,\Phi,e} \right\rangle
\end{aligned} \tag{59}$$

where $\tilde{\mathbf{F}}^{EXT,D}$ is the external body force and couple vector associated with free micromorphic FE nodal dofs in $\tilde{\mathcal{B}}^h$, $\tilde{\mathbf{F}}^{EXT,\hat{D}}$ the external body force and couple vector associated with prescribed micromorphic FE dofs in $\tilde{\mathcal{B}}^h$, where $\tilde{\mathbf{F}}^{EXT,D}$ and $\tilde{\mathbf{F}}^{EXT,\hat{D}}$ are extracted from $\tilde{\mathbf{F}}^{EXT,\check{D}}$, the total external body force and couple vector calculated in $\tilde{\mathcal{B}}^h$. $\hat{\mathbf{F}}^{EXT,\hat{D}}$ is the homogenized external body force and couple vector associated with prescribed micromorphic FE dofs in $\hat{\mathcal{B}}^h$, which has no contribution if $\hat{q} = 0$, i.e., underlying DNS body forces provide full contribution in $\hat{\mathcal{B}}^h$. $\tilde{\mathbf{F}}^{EXT,D}$ is the external force and couple vector associated with free micromorphic FE dofs in the pure micromorphic continuum FE domain $\tilde{\mathcal{B}}^h$.

3.2 Coupling approach 2:

In this coupling approach, it is also assumed that the micromorphic continuum-FE mesh covers the domain of the problem in which the bound particulate mechanics is not dominant, whereas in regions of significant grain-matrix debonding or intra-granular cracking leading to a macro-crack, a grain-scale mechanics representation is used in Fig.4.

In Fig.4, discrete domains are defined, where the yellow background denotes the DNS-FE overlap region \mathcal{B}^{DNS-FE} , with DNS region denoted by \mathcal{B}^{DNS} terminating at $\partial\mathcal{B}^{DNS}$, and micromorphic continuum FE region denoted by \mathcal{B}^{FE} terminating at $\partial\mathcal{B}^{FE}$.

3.2.1 3D Kinematics

The notation here for Coupling Approach 2 is similar to that used for Coupling Approach 1. We define a generalized dof vector \mathbf{Q} for all DNS nodal displacements in the system as

$$\mathbf{Q} = [\mathbf{q}_\alpha, \mathbf{q}_\beta, \dots, \mathbf{q}_\gamma]^T, \quad \alpha, \beta, \dots, \gamma \in \mathcal{A} \tag{60}$$

where \mathbf{q}_α is the displacement vector of DNS node α , and \mathcal{A} is the set of all DNS nodes. Likewise, the micromorphic finite element nodal displacements and micro-displacements are written as

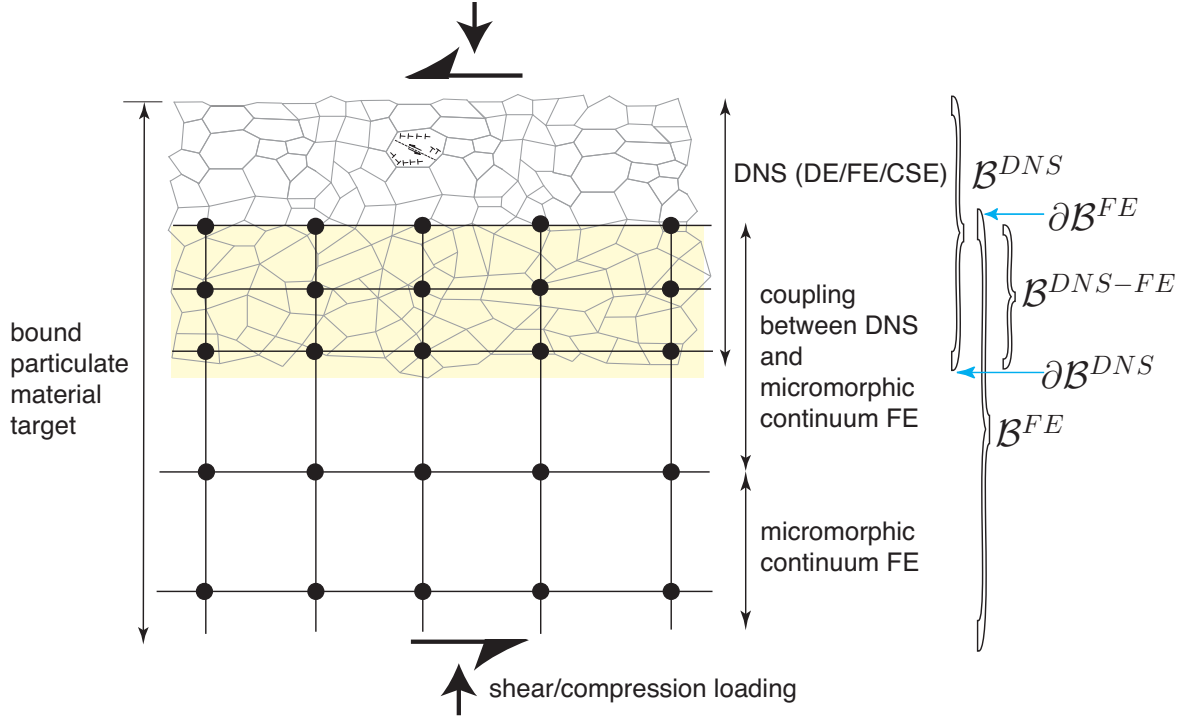


Figure 4. Two-dimensional illustration of Coupling Approach 2 between grain-FE DNS and micromorphic FE continuum regions.

$$\mathbf{D} = [\mathbf{d}_a, \mathbf{d}_b, \dots, \mathbf{d}_c, \phi_d, \phi_e, \dots, \phi_f]^T \quad (61)$$

$$a, b, \dots, c \in \mathcal{N}, \quad d, e, \dots, f \in \mathcal{M}$$

where \mathbf{d}_a is the displacement vector of node a , ϕ_d is the micro-displacement tensor in vector form of node d , \mathcal{N} is the set of all nodes, and \mathcal{M} is the set of micromorphic finite element nodes with micro-displacement tensor degrees of freedom, where $\mathcal{M} \subset \mathcal{N}$.

3.2.2 3D Kinetic and Potential Energy Partitioning and Coupling

For the DNS equations, the kinetic energy is T^Q , dissipation function F^Q , and potential energy U^Q , such that

$$\begin{aligned} T^Q &= \frac{1}{2} \dot{\mathbf{Q}} \mathbf{M}^Q \dot{\mathbf{Q}} \\ F^Q &= a_Q T^Q \\ U^Q(\mathbf{Q}) &= \int_0^{\mathbf{Q}} \mathbf{F}^{INT,Q}(\mathbf{S}) d\mathbf{S} \end{aligned} \quad (62)$$

where \mathbf{M}^Q is the mass matrix, and $\mathbf{F}^{INT,Q}$ is an internal force vector for the DNS region. For the micromorphic continuum FE equations, T^D is the kinetic energy, F^D the dissipation function, and U^D the potential energy, such that

$$\begin{aligned}
T^D &= \frac{1}{2} \dot{\mathbf{D}} \mathbf{M}^D \dot{\mathbf{D}} \\
F^D &= a_D T^D \\
U^D(\mathbf{D}) &= \int_0^{\mathbf{D}} \mathbf{F}^{INT,D}(\mathbf{S}) d\mathbf{S}
\end{aligned} \tag{63}$$

where \mathbf{M}^D is the mass and micro-inertia matrix, and $\mathbf{F}^{INT,D}$ is the internal force vector. We assume the total kinetic and potential energy and dissipation of the coupled DNS-micromorphic-continuum system may be written as the sum of the energies using the scalar distance function $\omega(\mathbf{X}) = \ell(\mathbf{X})/\ell_0$, where $\ell(\mathbf{X})$ is the orthogonal distance of point $\mathbf{X} \in \mathcal{B}^{DNS-FE}$ from $\partial\mathcal{B}^{FE}$, and ℓ_0 is the orthogonal length of \mathcal{B}^{DNS-FE} , such that

$$T(\dot{\mathbf{Q}}, \dot{\mathbf{D}}) = (1 - \omega)T^Q(\dot{\mathbf{Q}}) + \omega T^D(\dot{\mathbf{D}}) \tag{64}$$

$$U(\mathbf{Q}, \mathbf{D}) = (1 - \omega)U^Q(\mathbf{Q}) + \omega U^D(\mathbf{D}) \tag{65}$$

$$F(\dot{\mathbf{Q}}, \dot{\mathbf{D}}) = (1 - \omega)F^Q(\dot{\mathbf{Q}}) + \omega F^D(\dot{\mathbf{D}}) \tag{66}$$

Furthermore, the potential energy U of the coupled system is modified to include a constraint using a Lagrange multiplier, such that the Augmented-Lagrange multiplier constrained potential energy U_{AugLag} is written as

$$U_{\text{AugLag}} = U + \boldsymbol{\lambda} \cdot \mathbf{g} + \frac{1}{2} k \mathbf{g} \cdot \mathbf{g} \tag{67}$$

where $\boldsymbol{\lambda}$ is the vector of Lagrange multipliers (forces acting on DNS nodes in the overlap region), \mathbf{g} is the vector of constraints applied at each DNS node α within the overlap region, and k is a penalty parameter. The constraint at DNS node α in the overlap region is written as

$$\mathbf{g}_\alpha = (\mathbf{u}'_\alpha)^h(t) - \mathbf{q}_\alpha(t) = \mathbf{0} \tag{68}$$

where $(\mathbf{u}'_\alpha)^h(t)$ is the micro-continuum displacement at node α shown in Eq.(14). Lagrange's equations may then be stated as

$$\begin{aligned}
\frac{d}{dt} \left(\frac{\partial T}{\partial \dot{\mathbf{Q}}} \right) - \frac{\partial T}{\partial \mathbf{Q}} + \frac{\partial F}{\partial \dot{\mathbf{Q}}} + \frac{\partial U_{\text{AugLag}}}{\partial \mathbf{Q}} &= \mathbf{F}^{EXT,Q} \\
\frac{d}{dt} \left(\frac{\partial T}{\partial \dot{\mathbf{D}}} \right) - \frac{\partial T}{\partial \mathbf{D}} + \frac{\partial F}{\partial \dot{\mathbf{D}}} + \frac{\partial U_{\text{AugLag}}}{\partial \mathbf{D}} &= \mathbf{F}^{EXT,D}
\end{aligned} \tag{69}$$

which lead to a coupled system of governing equations (linear and first moment of momentum) for the coupled DNS-micromorphic-continuum mechanics. After taking the derivatives, and assuming mass and micro-inertia lumped matrices (for explicit dynamics), we arrive at the coupled system of equations to solve at DNS node α

$$\mathbf{A}_\alpha \left\{ (1 - \omega(\mathbf{X}_\alpha)) [m_\alpha^Q \ddot{\mathbf{q}}_\alpha + a_Q m_\alpha^Q \dot{\mathbf{q}}_\alpha + \mathbf{f}_\alpha^{INT,Q}(\mathbf{Q})] - \boldsymbol{\lambda}_\alpha - k \mathbf{g}_\alpha = \mathbf{f}_\alpha^{EXT,Q} \right\} \tag{70}$$

where m_α^Q is the lumped mass at DNS node α , $\mathbf{f}_\alpha^{INT,Q}$ is the internal force vector at DNS node α , $\mathbf{f}_\alpha^{EXT,Q}$ is the external force vector at DNS node α . For micromorphic FE node a , we have

$$\mathbf{A}_a \left\{ \omega(\mathbf{X}_a) \left[m_a^D \ddot{\mathbf{d}}_a + a_D m_a^D \dot{\mathbf{d}}_a + \mathbf{f}_a^{INT,D}(\mathbf{D}) \right] + \mathbf{A}_\alpha [N_a^u(\mathbf{X}_\alpha) (\boldsymbol{\lambda}_\alpha + k \mathbf{g}_\alpha)] = \mathbf{f}_a^{EXT,D} \right\} \quad (71)$$

where m_a^D is the lumped mass at micromorphic FE node a , $\mathbf{f}_a^{INT,D}$ is the internal force vector at micromorphic FE node a , $\mathbf{f}_a^{EXT,D}$ is the external force vector at micromorphic FE node a . For micromorphic FE node d , we have

$$\mathbf{A}_d \left\{ \omega(\mathbf{X}_d) \left[i_d^D \ddot{\boldsymbol{\phi}}_d + a_D i_d^D \dot{\boldsymbol{\phi}}_d + \mathbf{f}_d^{INT,D}(\mathbf{D}) \right] + \mathbf{A}_\alpha [N_d^\Phi(\mathbf{X}_\alpha) (\boldsymbol{\lambda}_\alpha + k \mathbf{g}_\alpha) \otimes \boldsymbol{\Xi}_\alpha^h] = \mathbf{f}_d^{EXT,D} \right\} \quad (72)$$

where i_d^D is the lumped micro-inertia at micromorphic FE node d .

An explicit time integration procedure and solution method is described in Xiao and Belytschko [2004], which can also be generalized for implicit time integration and a Newton-Raphson nonlinear solution procedure.

4 Overview of adaptivity approach

Numerical adaptivity is introduced to track, at the grain-scale, regions of dynamic material failure. An adaptive scheme can be considered in two ways to calculate conversion criteria: (a) using a calculated shear/compaction strain energy density averaged over a RVE of DNS micro-structure, and calculated at a Gauss point in a micromorphic FE; and (b) *a posteriori* model error estimators (e.g., Oden et al. [2006]). In terms of method development for conversion, we consider the cases illustrated in Fig.5 where a continuum micromorphic FE mesh region is converted to a particulate micro-structural DNS region, and vice versa. One of the challenges with this conversion is that we do not know the material micro-structure to make up the DNS region, nor its material parameters. We can use probability density functions (PDFs) to sample approximate grain size, shape, percentage of matrix versus grain material, inter-/intra-granular constitutive parameters, and grain-matrix interface de-bond strength, for instance. The sampling of PDFs will provide an initial guess for the DNS micro-structural geometry and material parameters. To ensure smooth conversion in terms of average stress, strain, and energy, we can calibrate inversely the material parameters (using the PDF sampling as an initial guess, and the DNS geometry fixed) through a micromorphic homogenization procedure.

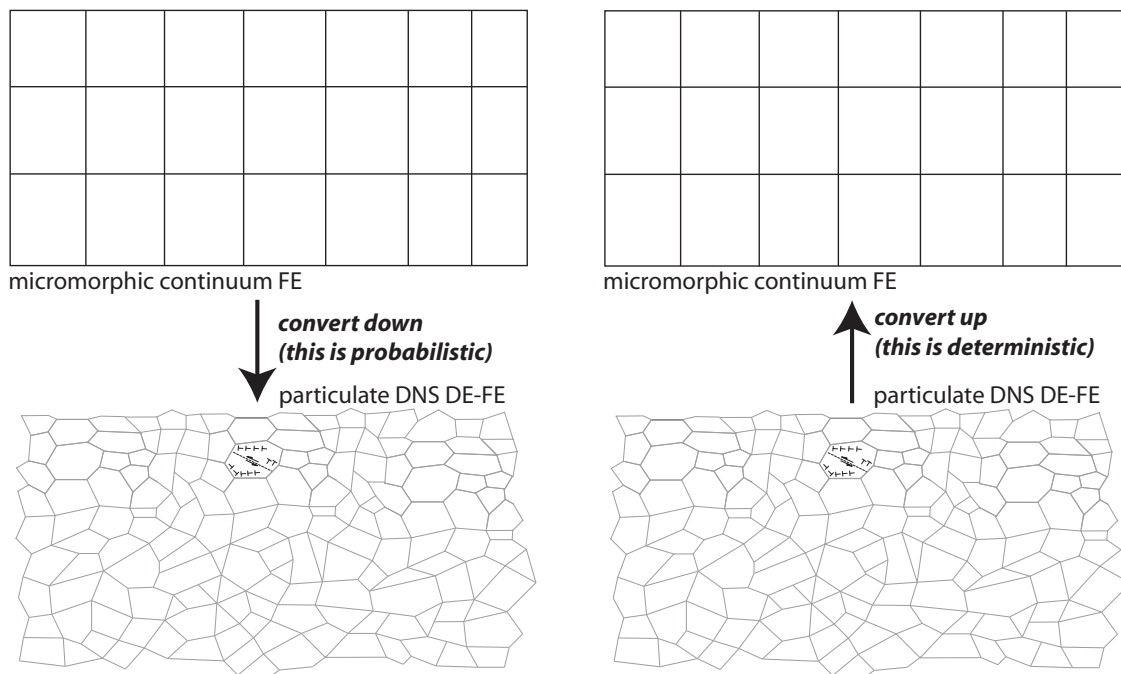


Figure 5. Adaptivity: conversion from micromorphic continuum FE to particulate DNS material model representation, and vice versa. The micromorphic continuum FE region could be the blue-dashed box at the bottom-center of the illustration in Fig.1 to be converted to a particulate DNS region for adaptive high-fidelity material modeling as the projectile penetrates the target. Note that since we do not know the exact particulate DNS configuration and material properties when converting from continuum FE to DNS in a region of potential fracture nucleation and fragmentation, this process is probabilistic, and thus PDFs will be used for the conversion.

We ended up not having time to implement these conversions illustrated in Fig.5.

5 Future Research

Future research entails the following: (1) extend the micromorphic 3D FE implementation to explicit dynamics in Tahoe; (2) implement the overlap procedures presented in Sect.3; and (3) test the adaptivity concepts presented in Sect.4.

Overall, the full 3D finite strain micromorphic coupled FE implementation and Drucker-Prager model formulation and implementation took longer than expected, but now it is nearly completed for the quasi-static case. The overlap coupling in 3D will continue after this project, to be supported by another project and to include the multiphase (solid, liquid, gas) nature of geologic and particulate materials. The adaptivity of our multiscale modeling approach will be investigated as part of future work, and it is still an important problem to investigate.

References

- V. Isbuga. Finite strain micromorphic finite element analysis of elastoplastic geomaterials. Phd thesis, University of Colorado at Boulder, 2012.
- V. Isbuga and R. Regueiro. Three-dimensional finite element analysis of finite strain micromorphic linear isotropic elasticity. *International Journal of Engineering Science*, 49: 1326–1336, 2011.
- V. Isbuga and R. Regueiro. Finite Element Analysis of Finite Strain Micromorphic Drucker-Prager Plasticity. *Int. J. Solids Struct.*, in review, 2012.
- H. Kadowaki and W.K. Liu. Bridging multi-scale method for localization problems. *Comp. Meth. App. Mech. Engr.*, 193(30-32):3267 – 3302, 2004.
- P.A. Klein and J.A. Zimmerman. Coupled atomistic-continuum simulations using arbitrary overlapping domains. *J. Comput. Phys.*, 213(1):86 – 116, 2006.
- J.T. Oden, S. Prudhomme, A. Romkes, and P.T. Bauman. Multiscale modeling of physical phenomena: adaptive control of models. *SIAM J. Sci. Comput.*, 28(6):2359–89, 2006.
- J.W.S. Rayleigh. *The Theory of Sound. Volume 1*. Dover Pub. Inc., New York, 1 edition, 1945.
- R. Regueiro and V. Isbuga. Length scale effects in finite strain micromorphic linear isotropic elasticity: Finite element analysis of three-dimensional cubical microindentation. *J. Nanoengineering and Nanosystems*, DOI: 10.1177/1740349911412850, 2011.
- R.A. Regueiro and B. Yan. Computational Homogenization and Partial Overlap Coupling Between Micropolar Elastic Continuum Finite Elements and Elastic Spherical Discrete Elements in one Dimension. In S. Li and X.-L. Gao, editors, *Handbook of Micromechanics and Nanomechanics*, volume 1, pages 1–45. Pan Stanford Pub., 2013.
- S.A. Silling. Reformulation of elasticity theory for discontinuities and long-range forces. *J. Mech. Phys. Solids*, 48(1):175 – 209, 2000.
- G.J. Wagner and W.K. Liu. Coupling of atomistic and continuum simulations using a bridging scale decomposition. *J. Comput. Phys.*, 190(1):249 – 74, 2003.
- S.P. Xiao and T. Belytschko. A bridging domain method for coupling continua with molecular dynamics. *Comp. Meth. App. Mech. Engr.*, 193(17-20):1645 – 69, 2004.